Change in structure between the $I = 1/2$ states in ^{181}Tl and ^{177,179}Au

J.G. Cubiss [a,b,*], A.E. Barzakh [c], A.N. Andreyev [a,d,b], M. Al Monthery [a], N. Althubiti [e],
B. Andel [f], S. Antalic [f], D. Atanasov [g], K. Blaum [g], T.E. Cocolios [h,e,b], T. Day Goodacre [b,e],
R.P. de Groote [h], A. de Roubin [g], G.J. Farooq-Smith [e,h], D.V. Fedorov [c], V.N. Fedosseev [b],
R. Ferrer [h], D.A. Fink [b,i], L.P. Gaffney [h], L. Ghys [h,j], A. Gredley [k], R.D. Harding [a,b], F. Herfurth [l],
M. Huyse [h], N. Imai [m], D.T. Joss [k], U. Köster [n], S. Kreim [b,g], V. Liberati [o], D. Lunney [p],
K.M. Lynch [b,e], V. Manea [b,p], B.A. Marsh [b], Y. Martinez Palenzuela [h], P.L. Molkanov [c],
P. Mosat [f], D. Neidherr [l], G.G. O'Neill [k], R.D. Page [k], T.J. Procter [b,e], E. Rapisarda [h,b],
M. Rosenbusch [q], S. Rothe [b,r], K. Sandhu [o], L. Schweikhard [q], M.D. Seliverstov [c], S. Sels [h],
P. Spagnoletti [o], V.L. Truesdale [a], C. Van Beveren [h], P. Van Duppen [h], M. Veinhard [b],
M. Venhart [s], M. Veselský [s], F. Wearing [k], A. Welker [b,t], F. Wienholtz [b,q], R.N. Wolf [q,g],
S.G. Zemlyanoy [u], K. Zuber [t]

[a] *Department of Physics, University of York, York, YO10 5DD, United Kingdom*
[b] *CERN, CH-1211 Geneva 23, Switzerland*
[c] *Petersburg Nuclear Physics Institute, NRC Kurchatov Institute, 188300 Gatchina, Russia*
[d] *Advanced Science Research Center (ASRC), Japan Atomic Energy Agency (JAEA), Tokai-mura, Ibaraki 319-1195, Japan*
[e] *School of Physics and Astronomy, The University of Manchester, Manchester, M13 9PL, United Kingdom*
[f] *Department of Nuclear Physics and Biophysics, Comenius University in Bratislava, 84248 Bratislava, Slovakia*
[g] *Max-Planck-Institut für Kernphysik, Saupfercheckweg 1, 69117 Heidelberg, Germany*
[h] *KU Leuven, Instituut voor Kern- en Stralingsfysica, B-3001 Leuven, Belgium*
[i] *Ruprecht-Karls Universität, D-69117 Heidelberg, Germany*
[j] *Belgian Nuclear Research Centre SCK•CEN, Boeretang 200, B-2400 Mol, Belgium*
[k] *Oliver Lodge Laboratory, University of Liverpool, Liverpool, L69 7ZE, United Kingdom*
[l] *GSI Helmholtzzentrum für Schwerionenforschung GmbH, 64291 Darmstadt, Germany*
[m] *High Energy Accelerator Research Organisation (KEK), Oho 1-1, Tsukuba, Ibaraki 305-0801, Japan*
[n] *Institut Laue Langevin, 6 rue Jules Horowitz, F-38042 Grenoble Cedex 9, France*
[o] *School of Engineering and Science, University of the West of Scotland, Paisley PA1 2BE, United Kingdom*
[p] *CSNSM-IN2P3-CNRS, Université Paris-Sud, 91406 Orsay, France*
[q] *Ernst-Moritz-Arndt-Universität, Institut für Physik, 17487 Greifswald, Germany*
[r] *Institut für Physik, Johannes Gutenberg-Universität Mainz, D-55128 Mainz, Germany*
[s] *Institute of Physics, Slovak Academy of Sciences, 845 11 Bratislava, Slovakia*
[t] *Technische Universität Dresden, 01069 Dresden, Germany*
[u] *Joint Institute of Nuclear Research, 141980 Dubna, Moscow Region, Russia*

ARTICLE INFO

ABSTRACT

The first accurate measurements of the α-decay branching ratio and half-life of the $I^\pi = 1/2^+$ ground state in ^{181}Tl have been made, along with the first determination of the magnetic moments and $I = 1/2$ spin assignments of the ground states in ^{177,179}Au. The results are discussed within the complementary systematics of the reduced α-decay widths and nuclear g factors of low-lying, $I^\pi = 1/2^+$ states in the neutron-deficient lead region. The findings shed light on the unexpected hindrance of the $1/2^+ \to 1/2^+$, ^{181}Tl$^g \to {}^{177}$Au^g α decay, which is explained by a mixing of $\pi 3s_{1/2}$ and $\pi 2d_{3/2}$ configurations in ^{177}Au^g, whilst ^{181}Tl^g remains a near-pure $\pi 3s_{1/2}$. This conclusion is inferred from the g factor of ^{177}Au^g which has an intermediate value between those of $\pi 3s_{1/2}$ and $\pi 2d_{3/2}$ states. A similar mixed configuration is

* Corresponding author.
 E-mail address: james.cubiss@york.ac.uk (J.G. Cubiss).

Gold nuclei
Thallium nuclei

proposed for the $I^\pi = 1/2^+$ ground state of ^{179}Au. This mixing may provide evidence for triaxial shapes in the ground states in these nuclei.

1. Introduction

Low-energy shape coexistence, whereby states of differing shape compete at low-excitation energies within the same nucleus, is an intriguing and complex facet of nuclear structure [1]. This phenomenon results from an interplay between two opposing behaviours: the stabilising effect of shell closures which preserves sphericity, and residual interactions between protons and neutrons that drive deformation [2]. However, the description of such behaviour remains a challenge for contemporary nuclear theory.

To simplify the description of this complex phenomenon, theoretical models often invoke axial and reflection symmetries. However, as highlighted in e.g. Ref. [3] for germanium isotopes, the use of such restrictions may lead to problems. In particular, coexisting energy minima at different quadrupole deformations could be connected by a valley of triaxiality, along which the true energy minimum lies. Therefore, special care should be taken when modelling nuclei that inhabit known or expected regions of triaxiality.

The neutron-deficient gold ($Z = 79$) isotopes have proved to be fertile ground for the study of shape coexistence and triaxiality [4–14]. The ground-state structures of odd-mass gold isotopes are seen to gradually evolve as the mass reduces down to $A = 187$ ($N = 108$). This is evidenced by their g factors, spins and parities which change from those of near-pure $\pi 2d_{3/2}$ configurations with $I^\pi = 3/2^+$ for the odd-A isotopes with $A \geqslant 191$, to mixed $\pi 2d_{3/2}/\pi 3s_{1/2}$ states with $I^\pi = 1/2^+$ in ^{187,189}Au [15,4]. However, these nuclei are seen to retain weakly oblate (near spherical) shapes. A more dramatic change in structure is seen below $A = 187$, with a large increase in the mean-squared charge radius indicating a sudden increase in the ground-state deformation [5–7]. This transition from weakly oblate to strongly prolate shapes makes these nuclei of particular interest for investigating coexisting structures within the region. The large increase in deformation is accompanied by a change in the ground-state configuration to the $5/2^-$ member of the band, based upon the strongly prolate $1/2[541]$ and/or $3/2[532]$ deformed states of a $\pi 1h_{9/2}$ parentage, as was proposed for ^{181,183,185}Au in Refs. [4,16,17]. The ground states of the neutron-deficient gold isotopes were predicted to stay strongly deformed until $A \approx 177$, where a return to near-spherical shapes was proposed to occur (see Fig. 31 in Ref. [18]). However, results from in-beam and α-decay studies suggest that this region of strong deformation ends earlier, at $A = 179$, where it is proposed that the ground state returns to a $\pi 2d_{3/2}/\pi 3s_{1/2}$ configuration [19–21].

Evidence for triaxial shapes has been found in the neighbouring platinum isotopes. In particular, the magnetic moments of the lowest $3/2^-$ states in the odd-A isotopes $^{187-193}$Pt were shown in Ref. [22] (see Fig. 6 therein) to have a strong dependence on the triaxial deformation parameter, γ. Gold isotopes, which can be viewed as a proton coupled to a platinum core, may also display such behaviour. Signatures of triaxiality have been seen in the excited states of some gold isotopes (see Refs. [23,11–13] and references within). Thus, it may be possible to observe signs of triaxiality in ground-state magnetic moments of gold nuclei, similar to those seen in the neighbouring platinum isotopes.

This article reports on a two-pronged experimental study of the ground and isomeric states of thallium and gold isotopes. First, an α-decay study of the $I = 1/2^+$ ground state in ^{181}Tl

($T_{1/2} = 3.2(3)$ s [24]) was performed to investigate the unexpected hindrance to the decay observed in a study by Andreyev et al. [25], at the velocity filter SHIP (GSI). In this work, the authors deduced an upper limit for the α-decay branching ratio of $b_\alpha(^{181}\text{Tl}^g) < 10\%$, which resulted in an upper limit for the reduced α-decay width of $\delta_\alpha^2 < 19$ keV. The latter is notably smaller than those of other unhindered $1/2^+ \rightarrow 1/2^+$ α decays in the region, which typically have values of $\delta_\alpha^2 = 45-90$ keV. This raises the question as to the possible cause of hindrance in the ^{181}Tl α decay. Recent mean-squared charge radii measurements by Barzakh et al. [26] show ^{181}Tl^g to be nearly spherical, with a magnetic moment in good agreement with values for the $I = 1/2^+$ states in other odd-A thallium isotopes, which have near-pure $\pi 3s_{1/2}$ configurations. This proves that there is nothing unusual with the underlying structure of ^{181}Tl^g. Therefore, the main goals of the present work were to extract a value for b_α and the half-life ($T_{1/2}$) of ^{181}Tl^g, in order to confirm or disprove the hindrance observed in Ref. [25].

On the other hand, a difference in configurations between ^{181}Tl^g and its α-decay daughter nucleus, ^{177}Au^g, could explain this hindrance. Prior to this work, ^{177}Au^g was tentatively assigned a spin of $I^\pi = (1/2^+, 3/2^+)$, based on the in-beam study by Kondev et al. [21], with the most likely configuration being either $1/2^+[411](d_{3/2})$ at oblate deformation with some admixture from $\pi 3s_{1/2}$, or a prolate $3/2^+[402](d_{3/2})$ state.

Therefore, in-source laser spectroscopy measurements of ^{177}Au^g were performed. The present work provides the first unambiguous measurements of the spins and magnetic moments of ^{177,179}Au^g. The new results for ^{181}Tl^g and ^{177,179}Au^g will be discussed within the context of the systematics of reduced α-decay widths for $1/2^+ \rightarrow 1/2^+$ α decays and nuclear g factors of $I = 1/2$ states within the region.

2. Experiment

Two experimental campaigns were performed for the isotopes ^{181}Tl^g and ^{177,179}Au^g. In both cases the experimental method was the same as that employed in the studies of the thallium isotopic chain presented in Refs. [26,27]. Additional details pertinent to the present work are given below. The radioactive thallium and gold nuclei were produced at the ISOLDE facility [28,29], in spallation reactions induced by a 1.4-GeV proton beam, impinged upon a 50 g/cm²-thick UC$_x$ target. The proton beam was delivered by the CERN PS Booster with an average current of 2.1 μA, in a repeated sequence known as a supercycle that typically consisted of 35–40, 2.4-μs long pulses, with a minimum interval of 1.2 s between each pulse.

After proton impact the reaction products diffused through the target matrix and effused towards a hot cavity ion source, kept at a temperature of $\approx 2000\,°$C. Inside the cavity, the thallium or gold atoms were selectively ionised by the ISOLDE Resonance Ionization Laser Ion Source (RILIS) [30,31]. The ions were then extracted from the cavity using a 30 kV electrostatic potential and separated according to their mass-to-charge ratio by the ISOLDE GPS mass separator. The mass-separated beam was then delivered to either the ISOLTRAP Multi-Reflection Time-of-Flight Mass Spectrometer (MR-ToF MS) [32] or the Windmill decay station [33,34], for photoion monitoring during RILIS laser-wavelength scans across the hyperfine structure (hfs) of an atomic transition used in the
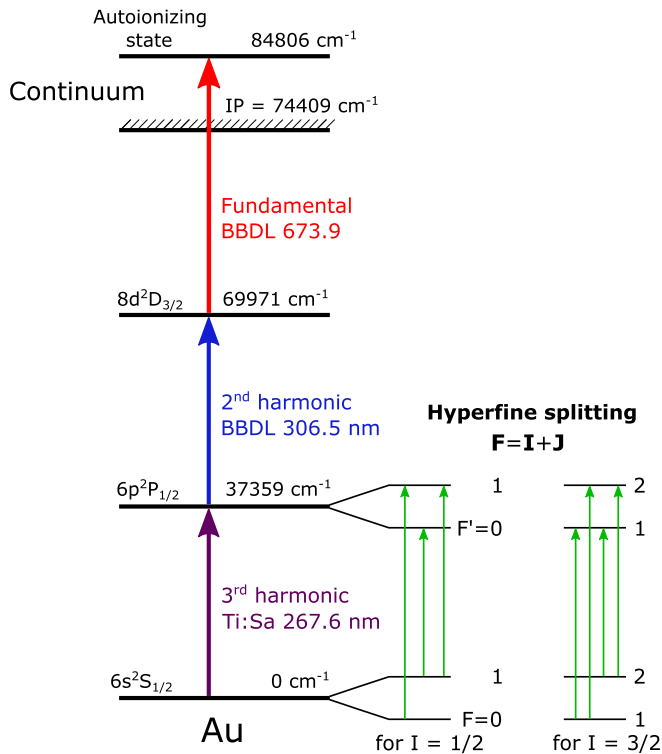
Fig. 1. The three-step resonant photoionization scheme used to produce gold ions [37], along with the hyperfine structures (not to scale) expected for a nucleus with spin $I = 1/2$, or $I = 3/2$. The green arrows indicate the allowed transitions between different electronic states: three lines for $I = 1/2$, and four for $I = 3/2$.

Fig. 2. Singles α-decay spectra recorded by (a) Si1, (b) Si2, (c) Si3 and (d) Si4, fitted with crystal ball (CB) functions. The red traces represent the convolution of CB functions fitted to the spectra, the blue traces are the individual components that contribute to the full fit. The peaks belonging to the α decays of ^{177}Pt, ^{181}Au, ^{181}Hg, ^{177}Au^g and ^{181}Tl^g are labelled, along with a weak, unidentified decay present in the Si1 and Si2 spectra, at $E_\alpha \approx 5750$ keV.

resonance ionization process (see Fig. 1). Details of the scanning procedures can be found in Ref. [35] for the MR-ToF MS, and Refs. [33,36] for the Windmill system.

As well as hfs scanning, the Windmill decay station was used for the decay studies of ^{181}Tl. The mass-separated beam entered the Windmill system through the central hole of an annular silicon detector (Si1) and was implanted into one of ten, 20 μg/cm^2-thick carbon foils mounted on a rotatable wheel. A second surface-barrier silicon detector (Si2) was positioned a few mm behind the foil at the implantation site. Together, Si1 + Si2 were used to measure the short-lived α activity at the implantation site. After a fixed number of supercycles the wheel of the Windmill was rotated within a 0.8 s time window, moving the irradiated foil to a decay site, between a pair of closely spaced silicon detectors (Si3 and Si4), which were used to measure long-lived decays. The full-width at half maxima of the recorded α-decay peaks were 22–35 keV, within the energy region of interest ($E_\alpha = $ 5000–7000 keV).

The α-decay study of ^{181}Tl^g was part of the experiment described in Ref. [26], in which the change in mean-squared charge radii and nuclear magnetic dipole moments of the thallium isotopic chain were discussed. During this experiment, a two-step resonant ionisation scheme was used to ionise the thallium isotopes. In the case of ^{181}Tl, only beams of the ground state were produced, as the production rate and half-life of the $I^\pi = 9/2^-$ isomer were too low for its extraction from the target ($T_{1/2} = 1.40(3)$ ms [19]).

In the separate experiment on ^{177,179}Au^g, the laser spectroscopy measurements were made using the three-step resonant ionisation scheme shown in Fig. 1 [37]. The IS and hfs measurements were made upon the 267.7-nm transition, by scanning a frequency-tripled titanium sapphire (Ti:Sa) laser in a narrowband mode (FWHM bandwidth of 600 MHz before tripling). Two broad-
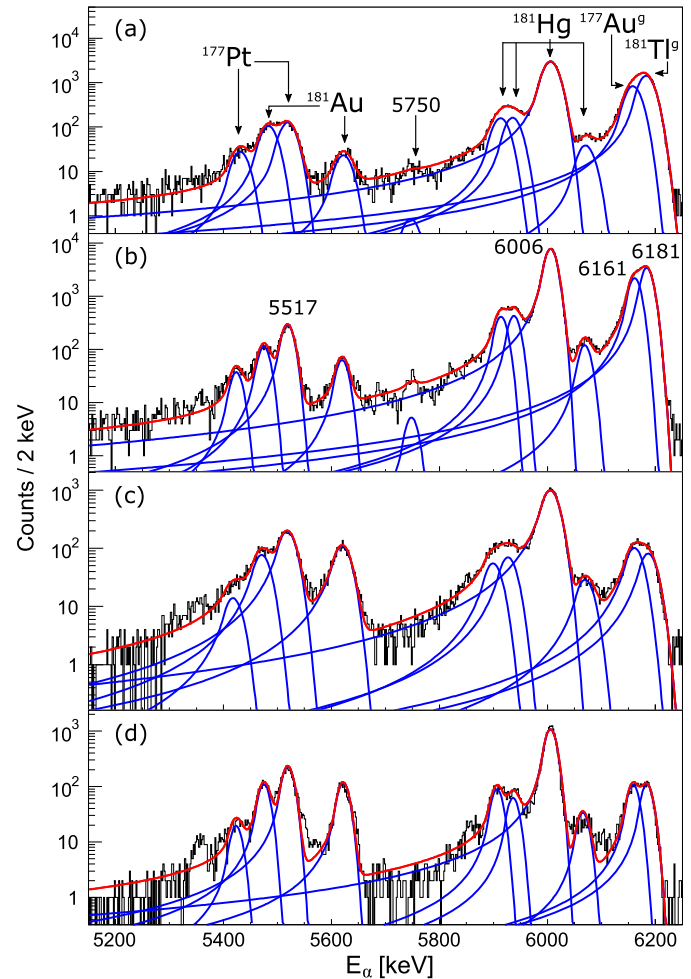
band dye lasers (BBDL; FWHM bandwidth of ≈20 GHz) were used for the second and third excitation steps.

3. Results

3.1. ^{181}Tl α-decay branching ratio and half-life

Fig. 2 shows the singles α-decay spectra recorded by the four silicon detectors of the Windmill system, during the α-decay study of ^{181}Tl^g. In the spectra, α decays originating from ^{181}Tl^g and its α-/β-decay daughter and granddaughter nuclei (^{181}Hg, ^{181}Au, ^{177}Au and ^{177}Pt) can be seen, along with an unidentified, low-intensity decay at $E_\alpha \approx 5750$ keV in the Si1 and Si2 spectra. Due to the long half-life of ^{181}Tl^g ($T_{1/2} = 3.2(3)$ s [24]), its α decays are also seen in Si3 and Si4 after the movement of the Windmill. Energy calibrations for the silicon detectors were made using the evaluated α-decay energies of ^{181}Hg ($E_\alpha = 6006(5)$ keV) and ^{177}Pt ($E_\alpha = 5517(4)$ keV) [38], both of which are part of the ^{181}Tl decay chain and were produced in the same run.

It is important to note the proximity in energy of the ^{177}Au^g and ^{181}Tl^g α decays, which differ by just ≈ 20 keV (see Fig. 2 and the following discussion). Because of this and their relatively long half-lives ($T_{1/2}(^{177}$Au$^g) = 1.462(32)$ s [21]), previous attempts

to extract values of b_α and $T_{1/2}$ from the mixed ^{181}Tl^g + ^{177}Au^g peak have had limited precision [39,40,24,19]. This issue is highlighted in Fig. 2, in which the energy peaks of the ^{181}Tl^g and ^{177}Au^g α decays are seen to overlap in all four spectra. This problem could be overcome by using the α–α correlation method for ^{181}Tl$^g \rightarrow \,^{177}$Au^g decays at recoil separators, but so far such studies have resulted in low statistics, making determination of the branching ratio difficult [40,24,19], with only an upper limit of $b_\alpha < 10\%$ reported in Ref. [25].

Despite this issue, it was possible to extract an accurate value of $b_\alpha(^{181}$Tl$^g)$ in the present work. This was done by fitting the singles α-decay spectra for each silicon detector separately, the results of which are shown by the red and blue curves in Fig. 2. The fitting was performed by the ROOT Minuit minimiser [41], using a binned-likelihood method and Crystal Ball functions [42–44] to describe the shape of the α-decay peaks. The parameters of the fits were left free, but kept such that those defining the tail and the width were the same for all peaks belonging to the spectrum of each individual detector. The fits yielded energies of $E_\alpha(^{181}$Tl$^g) = 6183(7)$ and $E_\alpha(^{177}$Au$^g) = 6159(7)$ keV. These values are in good agreement with those of Ref. [19]: $E_\alpha(^{181}$Tl$^g) = 6181(7)$ keV and $E_\alpha(^{177}$Au$^g) = 6161(7)$ keV, as well as Ref. [21] ($E_\alpha(^{177}$Au$^g) = 6160$ keV), where the isotope ^{177}Au^g was directly produced, and therefore the determination of E_α had no interference from the presence of ^{181}Tl^g.

The α-decay branching ratio of ^{181}Tl^g was determined by comparing the number of detected ^{181}Tl^g and ^{181}Hg α decays taken from the fits, corrected by the α-decay branching ratio of ^{181}Hg, such that

$$
\begin{aligned}
b_\alpha(^{181}\text{Tl}^g) &= \frac{100\% \times N_\alpha(^{181}\text{Tl}^g)}{N_\alpha(^{181}\text{Tl}^g) + N_\beta(^{181}\text{Tl}^g)} \\
&= \frac{100\% \times N_\alpha(^{181}\text{Tl}^g)}{N_\alpha(^{181}\text{Tl}^g) + \frac{N_\alpha(^{181}\text{Hg})}{b_\alpha(^{181}\text{Hg})}},
\end{aligned}
\tag{1}
$$

where $N_\alpha(X)$ represents the sum of the counts from all four silicon detectors, for a particular isotope. Using the evaluated value $b_\alpha(^{181}$Hg$) = 27(2)$ % [38], an α-decay branching ratio of $b_\alpha(^{181}$Tl$^g) = 8.6(6)$ % was deduced, which is in agreement with the upper limit of $b_\alpha(^{181}$Tl$^g) \leqslant 10$ % determined by Andreyev et al. [25].

A value of $T_{1/2}(^{181}$Tl$^g)$ was extracted from the combined decay curve recorded in Si3+Si4 (see Fig. 3). By selecting events belonging to the high-energy side of the combined ^{177}Au^g + ^{181}Tl^g peak ($6180 \leqslant E_\alpha \leqslant 6225$ keV, see Fig. 3 inset), the contribution of ^{177}Au^g α decays was < 10% of the total statistics. The extracted data were fitted with an exponential plus constant background, and a value of $T_{1/2}(^{181}$Tl$^g) = 2.9(1)$ s was extracted. This new value is in agreement with the literature value of $T_{1/2}(^{181}$Tl$^g) = 3.2(3)$ s [24] but is three times more precise.

The E_α, $T_{1/2}$ and b_α values extracted from the present data are compared with those from previous studies in Table 1. Using results from the current work and assuming $\Delta L = 0$ (see Sec. 3.2.1 for spin assignment of ^{177}Au^g), a value of $\delta_\alpha^2(^{181}$Tl$^g) = 17.9(18)$ keV was deduced using the Rasmussen approach [45].

3.2. Ground-state spins and magnetic dipole moments of ^{177,179}Au^g

3.2.1. Spins of ^{177,179}Au^g

Although ^{177}Au has two long-lived states ($T_{1/2} = 1462(32)$ ms and $E_\alpha = 6161(7)$ keV for the ground state, and $T_{1/2} = 1180(12)$ ms and $E_\alpha = 6124(7)$ keV for the isomeric state [21,19]), their respective hfs of the 267.6-nm transition do not overlap.
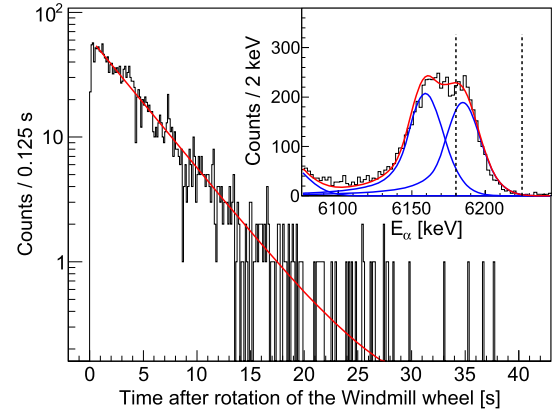

Fig. 3. Time distribution of $6180 \leqslant E_\alpha \leqslant 6225$-keV α decays, measured in Si3 and Si4, fitted with an exponential plus constant background function (red curve). The inset shows the sum of the singles-α decay spectra for Si3 and Si4, the blue and red curves are the sum of the fits shown in Figs. 2(c) and (d). The vertical, dashed lines indicate the gating conditions used to produce the decay curve shown in the main panel.

Table 1

Comparison of the E_α, $T_{1/2}$ and b_α values for the α decays of the ground states of ^{181}Tl and ^{177}Au extracted from the present work and previous studies.

Isotope	E_α [keV]	$T_{1/2}$ [s]	b_α [%]	δ_α^2 [keV]	Reference
^{181}Tl^g	6183(7)	2.9(1)	8.6(6)	17.9(18)	Present work
^{181}Tl^g	6181(7)	–	<10	<19[a]	[19]
^{181}Tl^g	6186(10)	3.2(3)	–	–	[24]

[a] Using $T_{1/2} = 3.2(3)$ s from Ref. [24].

Thus, with the laser tuned to the correct frequency, it is possible to obtain a clean ^{177}Au^g singles α-decay spectrum (see inset of Fig. 4(a), in which only the 6161-keV α decay of ^{177}Au^g is present). By gating on this peak, it was possible to extract a pure ^{177}Au^g hfs spectrum (Fig. 4(a)) from which a value of μ was deduced.[1]

The hfs spectrum for ^{177}Au^g, an example of which is shown in the main panel of Fig. 4(a), represents the measured α-decay rate as a function of the scanned laser frequency. The positions of the hyperfine components as a function of the scanning laser frequency are determined by the formula:

$$
\nu^{F,F'} = \nu_0 + a(6p) \cdot \frac{K'}{2} - a(6s) \cdot \frac{K}{2},
\tag{2}
$$

where ν_0 is the centroid frequency of the hfs, the prime symbol denotes the upper level of the atomic transition (see Fig. 1), $K = F(F+1) - I(I+1) - J(J+1)$, F is the quantum number for the total angular momentum of the atomic level, I and J are the quantum numbers for the nuclear spin and the angular momentum for the electronic state, respectively, and $a(nl)$ is the magnetic hyperfine coupling constant for the atomic level with the quantum numbers n and l.

As the upper and lower levels of the scanned transition both have $J = 1/2$, it is possible to distinguish between the two possibilities of nuclear spin, $I = 1/2$ and $I = 3/2$, by the number of peaks present in the hfs spectra shown in Fig. 4. For $I = 1/2$, the $F = 0 \rightarrow F' = 0$ excitation is forbidden. Therefore only three transitions are possible (see Fig. 1), with a hfs peak intensity profile of 1:2:1. In the case of $I = 3/2$, four peaks with a 5:5:1:5 relative intensity ratio would be expected (the blue arrows in Fig. 4

---

[1] The results for the isomeric state will be published elsewhere [46]. They confirm that the hfs of ^{177}Au^g and ^{177}Au^m do not overlap.

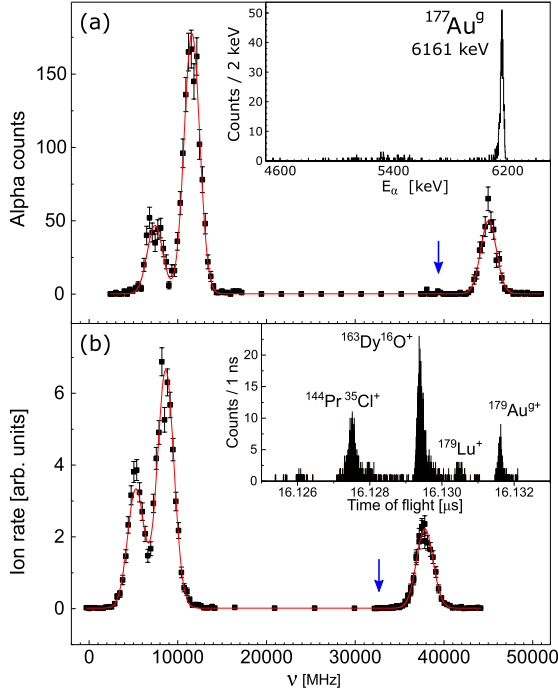**Fig. 4.** The hfs spectra for (a) ^{177}Au^g (Windmill) and (b) ^{179}Au^g (MR-ToF MS). The insets in panels (a) and (b) show the singles α-decay and the time-of-flight spectra recorded during the laser scans for ^{177}Au^g and ^{179}Au^g, measured by the Windmill and MR-ToF MS, respectively. Along with the ^{179}Au nuclei of interest, a number of mass contaminants can be seen in the $A = 179$ time-of-flight spectrum. In order to produce the hfs spectrum of ^{179}Au^g shown in panel (b), a ToF gate was placed upon its peak shown in the inset. The zero frequency corresponds to the hfs centroid of stable ^{197}Au^g. Both hfs spectra contain only three peaks, which firmly establishes that ^{177,179}Au^g have $I = 1/2$. The blue arrows indicate the approximate location a fourth peak would be expected, were $I(^{177,179}$Au$^g) = 3/2$ (see text for details).

approximate the expected position of the lowest-intensity peak in the case of $I = 3/2$). Thus, the three components of the hfs spectrum in Fig. 4(a) and the observed intensity ratios (similar to the expected 1:2:1 profile) unambiguously prove $I(^{177}$Au$^g) = 1/2$ (which justifies the use of $\Delta L = 0$ in the Rasmussen calculations of Sec. 3.1, for $I^\pi = 1/2^+$ ^{181}Tl^g [26]). The same situation is seen for ^{179}Au^g, the hfs of which also possesses three peaks and an intensity profile that prove it too has $I = 1/2$ (see Fig. 4(b)).

In passing we note that this new spin assignment for ^{179}Au^g, combined with the unhindered nature of its $E_\alpha = 5848(5)$ keV [38] α decay (see Fig. 5(a)), establishes a spin and parity of $I^\pi = 1/2^+$ for the state in the daughter nucleus ^{175}Ir that is fed by this α decay. Interestingly, previous in-beam studies did not find such a state and suggested that the ^{175}Ir ground state is $I^\pi = 5/2^-$ [47,48]. The structure of the low-lying states in ^{175}Ir will be further investigated in a forthcoming, dedicated decay study [49].

3.2.2. Magnetic dipole moments of ^{177,179}Au^g

The extracted hfs spectra were fitted using Voigt profiles [26], with $I = 1/2$, resulting in values of $a(6s,^{177}$Au$^g) =$ 66940(260) MHz and $a(6s,^{179}$Au$^g) = 58460(230)$ MHz.

To determine the magnetic moments, the prescription of Ekström et al. was used [4]:

$$\mu = \frac{a(6s)I}{29005} \pm 0.012, \quad \text{for } I = j = l \pm \frac{1}{2}. \tag{3}$$

This relationship takes into account the hyperfine anomaly [50], by application of the Moskowitz–Lombardi empirical rule [51]. This rule holds for single-particle shell model states with an orbital

angular momentum, l, and a total angular momentum, j. However, in a recent work by Frömmgen et al. [52], it was shown that the Moskowitz–Lombardi rule could not be applied to $I^\pi = 1/2^+$ states in cadmium isotopes. Analysis of the hyperfine anomaly for thallium isotopes with an odd proton in a $\pi 3s_{1/2}$ orbital shows that the correction factor of ± 0.012 in Eq. (3) should be replaced by a value of 0.05 [53]. The long-lived $I^\pi = 1/2^+$ states in gold isotopes can be an admixture of $\pi 3s_{1/2}(j = l + 1/2)$, and $\pi 2d_{3/2}(j = l - 1/2)$ states (see below). Therefore, a simplified version of Eq. (3) was used,[2] where the correction factor was removed and the uncertainty on μ was increased by 0.05, accordingly. This yields $\mu(^{177}$Au$^g) = 1.15(5)$ μ_N and $\mu(^{179}$Au$^g) = 1.01(5)$ μ_N.

4. Discussion

Fig. 5(a) shows the δ_α^2 values for $1/2^+ \rightarrow 1/2^+$ α decays, calculated using the Rasmussen approach [45], for gold ($Z = 79$, pink downwards triangles) [54–56,46], astatine ($Z = 85$, red circles) [57–61], bismuth ($Z = 83$, blue squares) [62,57,58,38,63], thallium ($Z = 81$, black triangles) [54,56] and iridium isotopes ($Z = 77$, teal crosses) [64,55,56,65]. The reader is reminded that unhindered α decays for odd-A nuclei within this region have typical values of $\delta_\alpha^2 = 45 - 90$ keV (indicated by the green, shaded region in Fig. 5(a)). In general terms, the δ_α^2 values decrease as $N \rightarrow 126$, due to a lowering of the α-particle preformation probability (see Refs. [66,67] for details). One sees this effect in the astatine and bismuth isotopes (as well as in the even-Z polonium, radon, radium and thorium isotopes, not shown in the plot). However, ^{181}Tl ($N = 100$) is far from the $N = 126$ shell closure and so this effect is not pertinent to the following discussion.

The value of $\delta_\alpha^2(^{181}$Tl$^g; 1/2 \rightarrow 1/2) = 17.9(18)$ keV deduced in the present work is smaller than typical $\delta_\alpha^2(1/2 \rightarrow 1/2)$ values in the region, in particular, those belonging to ^{177,179}Tl ($\delta_\alpha^2 = 56(19)$ and 50(3) keV, respectively) which are in good agreement with the observed systematics. A comparison of the δ_α^2 value of ^{181}Tl^g and the unhindered α decay of its even–even neighbour, ^{180}Hg,[3] yields a hindrance factor of HF$_\alpha = 4.1(5)$, indicating that the ^{181}Tl^g α decay is hindered. The mean-squared charge radii and magnetic moment results from Ref. [26] showed ^{181}Tl^g to be spherical, with a near-pure $\pi 3s_{1/2}$ configuration. These results are supported by potential energy surface (PES) calculations, made using the finite-range liquid drop model (FRDM) for the macroscopic part of the energy functional [71]. The results of these calculations for ^{181}Tl have a lowest-energy minimum that corresponds to a spherical nucleus (see Fig. 6). Thus, both the experimental results and the theoretical calculations show that there is nothing unusual with the structure of ^{181}Tl^g. Therefore, the observed hindrance in the ^{181}Tl^g α decay must be due to an unusual configuration in the daughter nucleus, ^{177}Au^g.

This configuration may be probed by investigating the g factor of ^{177}Au^g. In Fig. 5(b), the g factors for the $I = 1/2$ ground/isomeric states are plotted for gold (pink, downwards triangles [72] and references therein), astatine (red circles) [35], bismuth (blue squares) [73] and thallium (black triangles) [74–77,26] isotopes, along with those of the $I = 3/2$ ground states in gold nuclei (green diamonds) [72]. It is worth noting the remarkable constancy of the g factors as a function of neutron number for the thallium, bismuth and astatine isotopes. The data plotted in Fig. 5(b) show that the g factor for ^{181}Tl^g is in good agreement with those of other $I = 1/2$, odd-A thallium isotopes, as well as those of the astatine

---

[2] This is the same approach as used in Refs. [5–8,10].

[3] A value of $\delta_\alpha^2(^{180}$Hg$) = 74(4)$ keV was deduced for the unhindered ^{180}Hg decay, using data taken from Refs. [68–70].
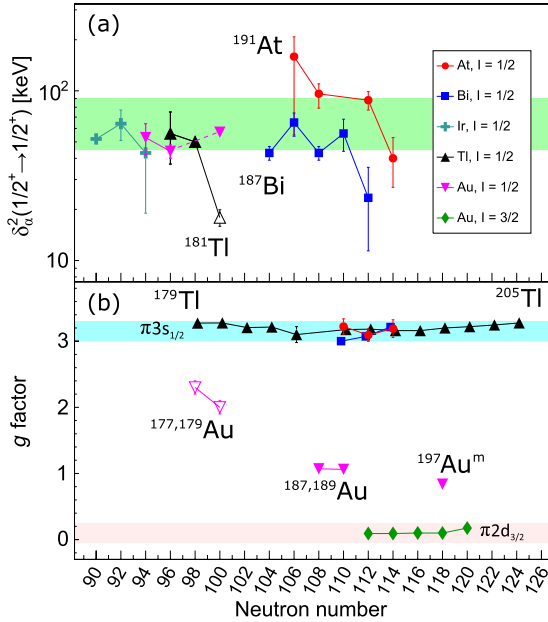
Fig. 5. (a) The reduced widths for $I = 1/2 \rightarrow 1/2$ α decays, the green shaded region represents $\delta_\alpha^2 = 45 - 90$ keV, typical of unhindered decays in odd-A isotopes in the region; (b) nuclear g factors, for $I = 1/2$ ground and isomeric states of isotopes surrounding the $Z = 82$ shell closure, along with the $I = 1/2$ (pink, downwards triangles) and $I = 3/2$ (green diamonds) states in gold isotopes, the blue and pink shaded regions represent the approximate g-factor values for near-pure $\pi 3s_{1/2}$ and $\pi 2d_{3/2}$ states, respectively. The hollow symbols for $\delta_\alpha^2(^{181}Tl^g)$ and $g(^{177,179}Au^g)$ are the results of the present work.

and bismuth chain. These nuclides, with $g \approx 3.2$, are characteristic of nuclei with a valence proton occupying a predominantly $\pi 3s_{1/2}$ orbital. In passing, we also note that the $I = 1/2$ states in the astatine and bismuth nuclei belong to weakly-deformed intruder configurations [73,35], whereas in thallium nuclei they are the normal, spherical states [26]. Thus, at least for small deformations, $g(\pi 3s_{1/2})$ is not sensitive to variations in the quadrupole deformation parameter, ϵ_2 (see also Ref. [78]).

In contrast to those of the near-pure $\pi 3s_{1/2}$ configurations in the thallium, bismuth and astatine isotopes, $g(^{177}Au^g)$ is noticeably smaller. This suggests that $^{177}Au^g$ has a different structure.

To understand this fact, we first note that the $I = 3/2$ states in $^{191-199}Au$ with $g \approx 0.1$ are dominated by a $\pi 2d_{3/2}$ configuration. All five measured g factors for the $I = 1/2$ states in $^{177,179,187,189,197}Au$ lie between the values of the $g(\pi 3s_{1/2})$ and $g(\pi 2d_{3/2})$ (see Fig. 5(b)). This indicates that these states have mixed $\pi 3s_{1/2}/\pi 2d_{3/2}$ configurations. The values of $g(^{187,189,197}Au; I = 1/2)$ are closer to those of the $I = 3/2$ states in heavier gold isotopes, which suggests their configurations are primarily $\pi 2d_{3/2}$. In contrast to this, the values of $g(^{177,179}Au^g)$ from the present work lie closer to those of $g(\pi 3s_{1/2})$, and appear to approach the latter with decreasing neutron number. This shift reveals a change in the dominant component of the wavefunction and a trend towards near-pure $\pi 3s_{1/2}$ configurations in the lightest gold isotopes. Furthermore, the hindrance in the $^{181}Tl^g \rightarrow {}^{177}Au^g$ α decay could be accounted for by a mixed $\pi 3s_{1/2}/\pi 2d_{3/2}$ configuration in $^{177}Au^g$ daughter nucleus, in comparison to the near-pure $\pi 3s_{1/2}$ configuration in $^{181}Tl^g$.

In order to better understand the structures of $^{177,179}Au^g$ it is instructive to explore the nature of the $I = 1/2$ states in $^{187,189}Au$ in more detail. The first measurement of $g(^{187}Au^g; I = 1/2) = 1.44(14)$ ($\mu = 0.72(7)$ μ_N) was made by Ekström et al. [4]. Particle-plus-Triaxial Rotor Model (PTRM) calculations showed that $g(^{187}Au^g; I = 1/2)$ has a high sensitivity to the degree of axial
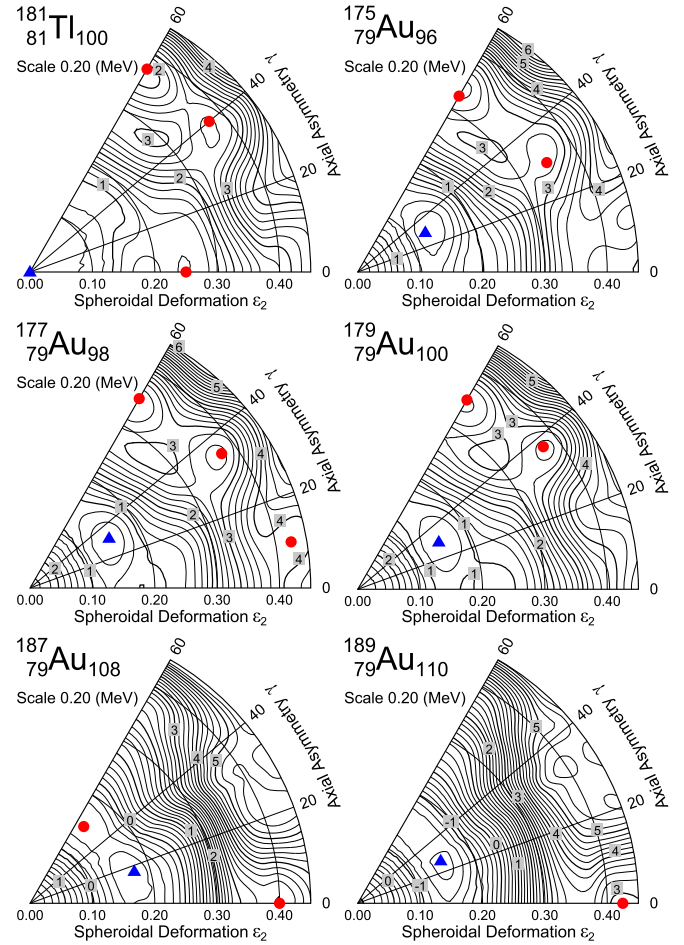

Fig. 6. Potential energy surface calculations for ^{181}Tl and $^{175,177,179,187,189}Au$ [71]. The blue triangles indicate the lowest-energy minimum, and the red spots other minima in the potential energy surfaces.

asymmetry, γ (see Fig. 7 in Ref. [4]). Using these calculations, the authors proposed that $^{187}Au^g$ was triaxial.

However, subsequent measurements performed by Wallmeroth et al. [7] (confirmed by Savard [8]) found $g(^{187}Au^g; I = 1/2) = 1.07(3)$ (shown in Fig. 5). Using the results from the PTRM calculations in Ref. [4], this new value was explained by a weak, oblate deformation, with no triaxiality (see discussion in Ref. [7]).

Further PTRM calculations were performed for $^{187,189}Au$, by Passler et al. [9], using combinations of quadrupole, hexadecapole and triaxial degrees of freedom, and modified oscillator or Woods-Saxon single-particle potentials. Again, the calculated g factors of $I = 1/2$ states were seen to be highly sensitive to variations in γ. The results of the calculations showed that the g factors of the $I = 1/2$ states in $^{187,189}Au$ were best described by weakly-oblate, axially-symmetric deformations, with some hexadecapole contribution, and mixed $\pi 3s_{1/2}/\pi 2d_{3/2}$ configurations.

In contrast to the PTRM results, the lowest-energy minima in the PES calculations for $^{187,189}Au$ are triaxial (see Fig. 6), albeit γ soft [71]. However, in the PES of ^{187}Au, there is another minimum at $\gamma \approx 55°$, $\epsilon_2 \approx 0.15$. This may correspond to the weakly-deformed, axially-symmetric oblate states proposed by Wallmeroth and Passler [7,9].

If one applies the same PTRM considerations used for $^{187,189}Au^g$ to $^{177,179}Au^g$, the results from the present work are best described by assuming $|\epsilon_2| \approx 0.18$ and $25° < \gamma < 30°$. Similar conclusions may be drawn from the PES plotted in Fig. 6, in which the lowest-

energy minima for ^{177,179}Au correspond to nuclei with $|\epsilon_2| \approx 0.15$, $\gamma \approx 30°$.

To summarise, the degree of mixing between $\pi 3s_{1/2}$ and $\pi 2d_{3/2}$ shell-model orbitals is crucial when describing the $I = 1/2$ states in the odd-A gold nuclei, with $A \leqslant 179$. Two completely different phenomena, reduced α-decay widths and magnetic dipole moments, point towards such mixed structures in ^{177,179}Au^g. This may also be an indication of triaxiality in these nuclei, however, a more rigorous theoretical interpretation is required. The use of beyond mean-field techniques may clarify the role of mixing between configurations of different deformations in cases with γ-soft minima in the PES, such as those of the present work.

5. Conclusion

In this study, the b_α and $T_{1/2}$ values of ^{181}Tl^g have been determined, along with spins and magnetic dipole moments of ^{177,179}Au^g. The results prove that the α decay of ^{181}Tl^g is hindered, which is surprising for a decay between states of equal spin. The reason for this hindrance is evident from the measured g factor of ^{177}Au^g, which lies between those of states dominated by a $\pi 3s_{1/2}$ or $\pi 2d_{3/2}$ orbital, indicating that ^{177}Au^g has a mixed $\pi 3s_{1/2}/\pi 2d_{3/2}$ configuration. Based on the similarity in their g factors, the $I = 1/2$ ground state of ^{179}Au is proposed to have a similar, mixed configuration to that of ^{177}Au^g.

The presence of mixed $\pi 3s_{1/2}/\pi 2d_{3/2}$ states could be a possible indication of triaxiality in the very neutron-deficient gold nuclei. However, further theoretical investigations are required to understand the relationship between these two phenomena. The highlighted interplay between mixing, triaxiality and shape coexistence is an important guide for constraining PES calculations that will accompany the next experimental step for g factor measurements for $N < 98$. Extending the measurements of magnetic dipole moments for $I = 1/2$ states in the gold nuclei further towards the proton drip line will help to elucidate whether they have mixed $\pi 3s_{1/2}/\pi 2d_{3/2}$ configurations, as in ^{177,179}Au^g, or if their structures evolve to near-pure $\pi 3s_{1/2}$ states. Indeed, results from α- and proton-decay studies of ^{171,173}Au suggest that they possess spherical, $I^\pi = 1/2^+$ ground states [54,79,80].

For example, the δ_α^2 value of the $I^\pi = 1/2^+$ state in ^{179}Tl matches well with those of other unhindered α decays (see Fig. 5), suggesting that ^{175}Au^g has a near-pure $\pi 3s_{1/2}$ configuration. However, the PES plot of ^{175}Au shown in Fig. 6 would suggest that the ground state of ^{175}Au is triaxial, and may have a similar structure to ^{177,179}Au^g. Thus, laser spectroscopy measurements of the $I = (1/2)$ state in ^{175}Au ($T_{1/2} = 207(7)$ ms [56]) are essential in gaining a better understanding of the evolving structures within the region. Such measurements are expected to be within the capabilities of current radioactive ion beam facilities.

Acknowledgements

References

[1] J.L. Wood, K. Heyde (Eds.), A focus on shape coexistence in nuclei, J. Phys. G, Nucl. Part. Phys. 43 (2016).

[2] K. Heyde, J.L. Wood, Shape coexistence in atomic nuclei, Rev. Mod. Phys. 83 (4) (2011) 1467–1521, https://doi.org/10.1103/RevModPhys.83.1467.

[3] L. Guo, J.A. Maruhn, P.-G. Reinhard, Triaxiality and shape coexistence in germanium isotopes, Phys. Rev. C 76 (3) (2007) 034317, https://doi.org/10.1103/PhysRevC.76.034317.

[4] C. Ekström, L. Robertsson, S. Ingelman, G. Wannberg, I. Ragnarsson, Nuclear ground-state spin of ^{185}Au and magnetic moments of ^{187,188}Au, Nucl. Phys. A 348 (1) (1980) 25–44, https://doi.org/10.1016/0375-9474(80)90543-6.

[5] K. Wallmeroth, G. Bollen, A. Dohn, P. Egelhof, J. Grüner, F. Lindenlauf, U. Krönert, J. Campos, A. Rodriguez Yunta, M.J.G. Borge, A. Venugopalan, J.L. Wood, R.B. Moore, H.J. Kluge, Sudden change in the nuclear charge distribution of very light gold isotopes, Phys. Rev. Lett. 58 (15) (1987) 1516–1519, https://doi.org/10.1103/PhysRevLett.58.1516.

[6] U. Krönert, S. Becker, G. Bollen, M. Gerber, T. Hilberath, H.J. Kluge, G. Passler, Observation of strongly deformed ground-state configurations in ^{184}Au and ^{183}Au by laser spectroscopy, Z. Phys. A At. Nucl. 331 (4) (1988) 521–522, https://doi.org/10.1007/BF01291911.

[7] K. Wallmeroth, G. Bollen, A. Dohn, P. Egelhof, U. Krönert, M.J.G. Borge, J. Campos, A. Rodriguez Yunta, K. Heyde, C. De Coster, J.L. Wood, H.-J. Kluge, Nuclear shape transition in light gold isotopes, Nucl. Phys. A 493 (2) (1989) 224–252, https://doi.org/10.1016/0375-9474(89)90396-5.

[8] G. Savard, J.E. Crawford, J.K.P. Lee, G. Thekkadath, H.T. Duong, J. Pinard, F. Le Blanc, P. Kilcher, J. Obert, J. Oms, J.C. Putaux, B. Roussiere, J. Sauvage, Laser spectroscopy of laser-desorbed gold isotopes, Nucl. Phys. A 512 (2) (1990) 241–252, https://doi.org/10.1016/0375-9474(90)93192-9.

[9] G. Passler, J. Rikovska, E. Arnold, H.-J. Kluge, L. Monz, R. Neugart, H. Ravn, K. Wendt, Quadrupole moments and nuclear shapes of neutron-deficient gold isotopes, Nucl. Phys. A 580 (2) (1994) 173–212, https://doi.org/10.1016/0375-9474(94)90769-2.

[10] F. Le Blanc, J. Obert, J. Oms, J.C. Putaux, B. Roussière, J. Sauvage, J. Pinard, L. Cabaret, H.T. Duong, G. Huber, M. Krieg, V. Sebastian, J. Crawford, J.K.P. Lee, J. Genevey, F. Ibrahim, Nuclear moments and deformation change in ^{184}Au^{g,m} from Laer spectroscopy, Phys. Rev. Lett. 79 (12) (1997) 2213–2216, https://doi.org/10.1103/PhysRevLett.79.2213.

[11] S.C. Wang, X.H. Zhou, Y.D. Fang, Y.H. Zhang, N.T. Zhang, B.S. Gao, M.L. Liu, J.G. Wang, F. Ma, Y.X. Guo, S.C. Li, X.L. Yan, L. He, Z.G. Wang, F. Fang, X.G. Wu, C.Y. He, Y. Zheng, Z.M. Wang, G.X. Dong, F.R. Xu, Level structure in the transitional nucleus ^{195}Au, Phys. Rev. C 85 (2) (2012) 027301, https://doi.org/10.1103/PhysRevC.85.027301.

[12] G.D. Dracoulis, G.J. Lane, H. Watanabe, R.O. Hughes, N. Palalani, F.G. Kondev, M.P. Carpenter, R.V.F. Janssens, T. Lauritsen, C.J. Lister, D. Seweryniak, S. Zhu, P. Chowdhury, W.Y. Liang, Y. Shi, F.R. Xu, Three-quasiparticle isomers and possible deformation in the transitional nuclide, ^{195}Au, Phys. Rev. C 87 (1) (2013) 014326, https://doi.org/10.1103/PhysRevC.87.014326.

[13] M. Venhart, F.A. Ali, W. Ryssens, J.L. Wood, D.T. Joss, A.N. Andreyev, K. Auranen, B. Bally, M. Balogh, M. Bender, R.J. Carroll, J.L. Easton, P.T. Greenlees, T. Grahn, P.-H. Heenen, A. Herzáň, U. Jakobsson, R. Julin, S. Juutinen, D. KÍč, J. Konki, E. Lawrie, M. Leino, V. Matoušek, C.G. McPeake, D. O'Donnell, R.D. Page, J. Pakarinen, J. Partanen, P. Peura, P. Rahkila, P. Ruotsalainen, M. Sandzelius, J. Sarén, B. Sayği, M. Sedlák, C. Scholey, J. Sorri, S. Stolze, A. Thornthwaite, J. Uusitalo, M. Veselský, De-excitation of the strongly coupled band in ^{177}Au and implications for core intruder configurations in the light Hg isotopes, Phys. Rev. C 95 (6) (2017) 061302, https://doi.org/10.1103/PhysRevC.95.061302.

[14] M. Venhart, J.L. Wood, M. Sedlák, M. Balogh, M. Bírová, A.J. Boston, T.E. Cocolios, L.J. Harkness-Brennan, R.-D. Herzberg, L. Holub, D.T. Joss, D.S. Judson, J. Kliman, J. Klimo, L. Krupa, J. Lušnák, L. Makhathini, V. Matoušek, Š. Motyčák, R.D. Page, A. Patel, K. Petrík, A.V. Podshibyakin, P.M. Prajapati, A.M. Rodin, A. Špaček, R. Urban, C. Unsworth, M. Veselský, New systematic features in the neutron-deficient Au isotopes, J. Phys. G, Nucl. Part. Phys. 44 (7) (2017) 074003, https://doi.org/10.1088/1361-6471/aa7297.

[15] C. Ekström, I. Lindgren, S. Ingelman, M. Olsmats, G. Wannberg, Nuclear spins of ^{186,187,188,189,189m}Au, Phys. Lett. B 60 (2) (1976) 146–148, https://doi.org/10.1016/0370-2693(76)90409-3, URL http://linkinghub.elsevier.com/retrieve/pii/0370269376904093.

[16] M.I. Macias-Marques, C. Bourgeois, P. Kilcher, B. Roussière, J. Sauvage, M.C. Abreu, M.G. Porquet, Decays of ^{183}Hg and ^{183}Au, Nucl. Phys. A 427 (2) (1984) 205–223, https://doi.org/10.1016/0375-9474(84)90082-4.

[17] J. Sauvage, C. Bourgeois, P. Kilcher, F. Le Blanc, B. Roussière, M. Macias-Marques, F. Bragança Gil, H. Porquet, H. Dautet, Decays of ^{181}Hg ($T_{1/2} = 3.6$ s) and

[181]Au (T$_{1/2}$ = 11.4 s), and low-spin states of [181]Pt and [177,181]Ir, Nucl. Phys. A 540 (1–2) (1992) 83–116, https://doi.org/10.1016/0375-9474(92)90196-Q.

[18] J.L. Wood, E.F. Zganjar, C. De Coster, K. Heyde, Electric monopole transitions from low energy excitations in nuclei, Nucl. Phys. A 651 (4) (1999) 323–368, https://doi.org/10.1016/S0375-9474(99)00143-8.

[19] A.N. Andreyev, S. Antalic, D. Ackermann, T.E. Cocolios, V.F. Comas, J. Elseviers, S. Franchoo, S. Heinz, J.A. Heredia, F.P. Heßberger, S. Hofmann, M. Huyse, J. Khuyagbaatar, I. Kojouharov, B. Kindler, B. Lommel, R. Mann, R.D. Page, S. Rinta-Antila, P.J. Sapple, Š. Šáro, P.V. Duppen, M. Venhart, H.V. Watkins, Decay of the 9/2^{-} isomer in [181]Tl and mass determination of low-lying stats in [181]Tl, [177]Au, and [173]Ir, Phys. Rev. C 80 (2) (2009) 024302, https://doi.org/10.1103/PhysRevC.80.024302.

[20] M. Venhart, A.N. Andreyev, J.L. Wood, S. Antalic, L. Bianco, P.T. Greenlees, U. Jakobsson, P. Jones, R. Julin, S. Juutinen, S. Ketelhut, M. Leino, M. Nyman, R.D. Page, P. Peura, P. Rahkila, J. Sarén, C. Scholey, J. Sorri, J. Thomson, J. Uusitalo, Shape coexistence in odd-mass Au isotopes: determination of the excitation energy of the lowest intruder state in [179]Au, in: Elementary Particle and High-Energy Physics, Phys. Lett. B 695 (1–4) (2011) 82–87, https://doi.org/10.1016/j.physletb.2010.10.055.

[21] F.G. Kondev, M.P. Carpenter, R.V.F. Janssens, K. Abu Saleem, I. Ahmad, H. Amro, J.A. Cizewski, M. Danchev, C.N. Davids, D.J. Hartley, A. Heinz, T.L. Khoo, T. Lauritsen, C.J. Lister, W.C. Ma, G.L. Poli, J. Ressler, W. Reviol, L.L. Riedinger, D. Seweryniak, M.B. Smith, I. Wiedenhöver, Identification of excited structures in proton unbound nuclei [173,175,177]Au: shape co-existence and intruder bands, Phys. Lett. B 512 (3–4) (2001) 268–276, https://doi.org/10.1016/S0370-2693(01)00714-6.

[22] T. Hilberath, S. Becker, G. Bollen, H.J. Kluge, U. Kronert, G. Passler, J. Rikovska, R. Wyss, Ground-state properties of neutron-deficient platinum isotopes, Z. Phys. A, Hadrons Nucl. 342 (1) (1992) 1–15, https://doi.org/10.1007/BF01294481.

[23] Y. Oktem, D.L. Balabanski, B. Akkus, L.A. Susam, L. Atanasova, C.W. Beausang, R.B. Cakirli, R.F. Casten, M. Danchev, M. Djongolov, E. Ganioğlu, K.A. Gladnishki, J.T. Goon, D.J. Hartley, A. Aecht, R. Krücken, J.R. Novak, G. Rainovski, L.L. Riedinger, T. Venkova, I. Yigitoglu, N.V. Zamfir, O. Zeidan, Triaxial deformation and nuclear shape transition in [192]Au, Phys. Rev. C 86 (5) (2012) 054305, https://doi.org/10.1103/PhysRevC.86.054305.

[24] K.S. Toth, X.-J. Xu, C.R. Bingham, J.C. Batchelder, L.F. Conticchio, W.B. Walters, L.T. Brown, C.N. Davids, R.J. Irvine, D. Seweryniak, J. Wauters, E.F. Zganjar, Phys. Rev. C 58 (2) (1998) 1310–1313, https://doi.org/10.1103/PhysRevC.58.1310.

[25] A.N. Andreyev, D. Ackermann, F.P. Heßberger, K. Heyde, S. Hofmann, M. Huyse, D. Karlgren, I. Kojouharov, B. Kindler, B. Lommel, G. Münzenberg, R.D. Page, K. Van de Vel, P. Van Duppen, W.B. Walters, R. Wyss, Shape-changing particle decays of [185]Bi and structure of the lightest odd-mass Bi isotopes, Phys. Rev. C 69 (5) (2004) 054308, https://doi.org/10.1103/PhysRevC.69.054308.

[26] A.E. Barzakh, A.N. Andreyev, T.E. Cocolios, R.P. de Groote, D.V. Fedorov, V.N. Fedosseev, R. Ferrer, D.A. Fink, L. Ghys, M. Huyse, U. Köster, J. Lane, V. Liberati, K.M. Lynch, B.A. Marsh, P.L. Molkanov, T.J. Procter, E. Rapisarda, S. Rothe, K. Sandhu, M.D. Seliverstov, A.M. Sjödin, C. Van Beveren, P. Van Duppen, M. Venhart, M. Veselský, Changes in mean-squared charge radii and magnetic moments of [179-184]Tl measured by in-source laser spectroscopy, Phys. Rev. C 95 (1) (2017) 014324, https://doi.org/10.1103/PhysRevC.95.014324.

[27] C. Van Beveren, A.N. Andreyev, A.E. Barzakh, T.E. Cocolios, R.P.D. Groote, D. Fedorov, V.N. Fedosseev, R. Ferrer, L. Ghys, M. Huyse, U. Köster, J. Lane, V. Liberati, K.M. Lynch, B.A. Marsh, P.L. Molkanov, T.J. Procter, E. Rapisarda, K. Sandhu, M.D. Seliverstov, P.V. Duppen, M. Venhart, M. Veselský, α-decay study of [182,184]Tl, J. Phys. G, Nucl. Part. Phys. 43 (2) (2016) 025102, https://doi.org/10.1088/0954-3899/43/2/025102.

[28] E. Kugler, The ISOLDE facility, Hyperfine Interact. 129 (1/4) (2000) 23–42, https://doi.org/10.1023/A:1012603025802.

[29] R. Catherall, W. Andreazza, M. Breitenfeldt, A. Dorsival, G.J. Focker, T.P. Gharsa, T.J. Giles, J.-L. Grenard, F. Locci, P. Martins, S. Marzari, J. Schipper, A. Shornikov, T. Stora, The ISOLDE facility, J. Phys. G, Nucl. Part. Phys. 44 (9) (2017) 094002, https://doi.org/10.1088/1361-6471/aa7eba.

[30] V. Mishin, V. Fedoseyev, H.-J. Kluge, V. Letokhov, H. Ravn, F. Scheerer, Y. Shirakabe, S. Sundell, O. Tengblad, Chemically selective laser ion-source for the CERN-ISOLDE on-line mass separator facility, Nucl. Instrum. Methods Phys. Res., Sect. B, Beam Interact. Mater. Atoms 73 (4) (1993) 550–560, https://doi.org/10.1016/0168-583X(93)95839-W.

[31] V. Fedosseev, K. Chrysalidis, T.D. Goodacre, B. Marsh, S. Rothe, C. Seiffert, K. Wendt, Ion beam production and study of radioactive isotopes with the laser ion source at ISOLDE, J. Phys. G, Nucl. Part. Phys. 44 (8) (2017) 084006, https://doi.org/10.1088/1361-6471/aa78e0.

[32] R.N. Wolf, F. Wienholtz, D. Atanasov, D. Beck, K. Blaum, C. Borgmann, F. Herfurth, M. Kowalska, S. Kreim, Y.A. Litvinov, D. Lunney, V. Manea, D. Neidherr, M. Rosenbusch, L. Schweikhard, J. Stanja, K. Zuber, ISOLTRAP's multi-reflection time-of-flight mass separator/spectrometer, Int. J. Mass Spectrom. 349–350 (1) (2013) 123–133, https://doi.org/10.1016/j.ijms.2013.03.020.

[33] H. De Witte, A.N. Andreyev, N. Barre, M. Bender, T.E. Cocolios, S. Dean, D. Fedorov, V.N. Fedosseev, L.M. Fraile, S. Franchoo, V. Hellemans, P.H. Heenen, K. Heyde, G. Huber, M. Huyse, H. Jeppessen, U. Köster, P. Kunz, S.R. Lesher, B.A. Marsh, I. Mukha, B. Roussière, J. Sauvage, M. Seliverstov, I. Stefanescu, E. Tengborn, K. Van De Vel, J. Van De Walle, P. Van Duppen, Y. Volkov, Nuclear charge radii of neutron-deficient lead isotopes beyond N = 104 midshell investigated by in-source laser spectroscopy, Phys. Rev. Lett. 98 (11) (2007) 16, https://doi.org/10.1103/PhysRevLett.98.112502.

[34] A.N. Andreyev, J. Elseviers, M. Huyse, P. Van Duppen, S. Antalic, A. Barzakh, N. Bree, T.E. Cocolios, V.F. Comas, J. Diriken, D. Fedorov, V. Fedosseev, S. Franchoo, J.A. Heredia, O. Ivanov, U. Köster, B.A. Marsh, K. Nishio, R.D. Page, N. Patronis, M. Seliverstov, I. Tsekhanovich, P. Van Den Bergh, J. Van De Walle, M. Venhart, S. Vermote, M. Veselsky, C. Wagemans, T. Ichikawa, A. Iwamoto, P. Möller, A.J. Sierk, et al., New type of asymmetric fission in proton-rich nuclei, Phys. Rev. Lett. 105 (25) (2010) 1, https://doi.org/10.1103/PhysRevLett.105.252502.

[35] J.G. Cubiss, A.E. Barzakh, M.D. Seliverstov, A.N. Andreyev, B. Andel, S. Antalic, P. Ascher, D. Atanasov, D. Beck, J. Bieroń, K. Blaum, C. Borgmann, M. Breitenfeldt, L. Capponi, T.E. Cocolios, T. Day Goodacre, X. Derkx, H. De Witte, J. Elseviers, D. Fedorov, V.N. Fedosseev, S. Fritzsche, L.P. Gaffney, S. George, L. Ghys, F.P. Heßberger, M. Huyse, N. Imai, Z. Kalaninová, D. Kisler, U. Köster, M. Kowalska, S. Kreim, J.F.W. Lane, V. Liberati, D. Lunney, K.M. Lynch, V. Manea, B.A. Marsh, S. Mitsuoka, P.L. Molkanov, Y. Nagame, D. Neidherr, K. Nishio, S. Ota, D. Pauwels, L. Popescu, D. Radulov, E. Rapisarda, J.P. Revill, M. Rosenbusch, R.E. Rossel, S. Rothe, K. Sandhu, L. Schweikhard, S. Sels, V.L. Truesdale, C. Van Beveren, P. Van den Bergh, Y. Wakabayashi, P. Van Duppen, K.D.A. Wendt, F. Wienholtz, B.W. Whitmore, G.L. Wilson, R.N. Wolf, K. Zuber, Charge radii and electromagnetic moments of [195-211]At, Phys. Rev. C 97 (5) (2018) 054327, https://doi.org/10.1103/PhysRevC.97.054327.

[36] M.D. Seliverstov, T.E. Cocolios, W. Dexters, A.N. Andreyev, S. Antalic, A.E. Barzakh, B. Bastin, J. Büscher, I.G. Darby, D.V. Fedorov, V.N. Fedosseev, K.T. Flanagan, S. Franchoo, G. Huber, M. Huyse, M. Keupers, U. Köster, Y. Kudryavtsev, B.A. Marsh, P.L. Molkanov, R.D. Page, A.M. Sjödin, I. Stefan, P. Van Duppen, M. Venhart, S.G. Zemlyanoy, Electromagnetic moments of odd-A [193-203,211]Po isotopes, Phys. Rev. C 89 (3) (2014) 034323, https://doi.org/10.1103/PhysRevC.89.034323.

[37] B.A. Marsh, V.N. Fedosseev, P. Kosuri, Development of a RILIS ionisation scheme for gold at ISOLDE, CERN, Hyperfine Interact. 171 (1–3) (2006) 109–116, https://doi.org/10.1007/s10751-006-9498-8.

[38] NNDC, Evaluated nuclear structure data file, Evaluated Nuclear Structure Data File.

[39] V.A. Bolshakov, A.G. Dernjatin, K.A. Mezilev, Y.N. Novikov, A.V. Popov, Y.Y. Sergeev, V.I. Tikhonov, V.A. Sergienko, G.V. Veselov, in: Nuclei Far from Stability/Atomic Masses and Fundamental Constans 1992, 6th International Conference on Nuclei Far from Stability (NFFS 6) Jointly with 9th International Conference on Atomic Masses and Fundamental Constants (AMCO 9) Bernkastel-Kues, Germany, July 19–25, 1992, 1992.

[40] K.S. Toth, J.C. Batchelder, C.R. Bingham, L.F. Conticchio, W.B. Walters, C.N. Davids, D.J. Henderson, R. Herman, H. Penttilä, J.D. Richards, A.H. Wuosmaa, B.E. Zimmerman, α-decay properties of [181]Pb, Phys. Rev. C 53 (5) (1996) 2513–2515, https://doi.org/10.1103/PhysRevC.53.2513.

[41] F. James, M. Roos, Minuit – a system for function minimization and analysis of the parameter errors and correlations, Comput. Phys. Commun. 10 (6) (1975) 343–367, https://doi.org/10.1016/0010-4655(75)90039-9.

[42] M.J. Oreglia, A study of the reactions psi prime –> gamma gamma psi, Ph.D. Thesis, SLAC-R-236.

[43] J.E. Gaiser, Charmonium spectroscopy from radiative decays of the j/psi and psi-prime, Ph.D. Thesis, SLAC-R-255.

[44] T. Skwarnicki, A study of the radiative cascade transitions between the upsilon-prime and upsilon resonances, Ph.D Thesis, DESY F31-86-02.

[45] J.O. Rasmussen, Alpha-decay barrier penetrabilities with an exponential nuclear potential: even–even nuclei, Phys. Rev. 113 (6) (1959) 1593–1598, https://doi.org/10.1103/PhysRev.113.1593.

[46] R.D. Harding, et al., unpublished.

[47] G.D. Dracoulis, B. Fabricius, T. Kibedi, A.M. Baxter, A.P. Byrne, K.P. Lieb, A.E. Stuchbery, Spectroscopy of [175]Ir and [177]Ir and deformation effects in odd iridium nuclei, Nucl. Phys. A 534 (1) (1991) 173–203, https://doi.org/10.1016/0375-9474(91)90562-K.

[48] B. Cederwall, B. Fant, R. Wyss, A. Johnson, J. Nyberg, J. Simpson, A.M. Bruce, J.N. Mo, High-spin states of [175]Ir: quasiproton-induced shapes and extreme, Phys. Rev. C 43 (5) (1991) R2031–R2034, https://doi.org/10.1103/PhysRevC.43.R2031.

[49] S.D. Gillespie, et al., unpublished.

[50] A. Bohr, V.F. Weisskopf, The influence of nuclear structure on the hyperfine structure of heavy elements, Phys. Rev. 77 (1) (1950) 94–98, https://doi.org/10.1103/PhysRev.77.94.

[51] P. Moskowitz, M. Lombardi, Distribution of nuclear magnetization in mercury isotopes, Phys. Lett. B 46 (3) (1973) 334–336, https://doi.org/10.1016/0370-2693(73)90132-9.

[52] N. Frömmgen, D.L. Balabanski, M.L. Bissell, J. Bieroń, K. Blaum, B. Cheal, K. Flanagan, S. Fritzsche, C. Geppert, M. Hammen, M. Kowalska, K. Kreim,

A. Krieger, R. Neugart, G. Neyens, M.M. Rajabali, W. Nörtershäuser, J. Papuga, D.T. Yordanov, Collinear laser spectroscopy of atomic cadmium, Eur. Phys. J. D 69 (6) (2015) 164, https://doi.org/10.1140/epjd/e2015-60219-0, URL http://link.springer.com/10.1140/epjd/e2015-60219-0.

[53] J.R. Persson, Table of hyperfine anomaly in atomic systems, At. Data Nucl. Data Tables 99 (1) (2013) 62–68, https://doi.org/10.1016/j.adt.2012.04.002.

[54] G.L. Poli, C.N. Davids, P.J. Woods, D. Seweryniak, J.C. Batchelder, L.T. Brown, C.R. Bingham, M.P. Carpenter, L.F. Conticchio, T. Davinson, J. DeBoer, S. Hamada, D.J. Henderson, R.J. Irvine, R.V.F. Janssens, H.J. Maier, L. Muller, F. Soramel, K.S. Toth, W.B. Walters, J. Wauters, Proton and alpha radioactivity below the $Z = 82$ shell closure, Phys. Rev. C 59 (6) (1999) R2979–R2983, https://doi.org/10.1103/PhysRevC.59.R2979.

[55] A. Thornthwaite, D. O'Donnell, R.D. Page, D.T. Joss, C. Scholey, L. Bianco, L. Capponi, R.J. Carroll, I.G. Darby, L. Donosa, M.C. Drummond, F. Ertuğral, T. Grahn, P.T. Greenlees, K. Hauschild, A. Herzan, U. Jakobsson, P. Jones, R. Julin, S. Juutinen, S. Ketelhut, M. Labiche, M. Leino, A. Lopez-Martens, K. Mullholland, P. Nieminen, P. Peura, P. Rahkila, S. Rinta-Antila, M. Sandzelius, J. Sarén, B. Sayği, J. Simpson, J. Sorri, J. Uusitalo, Characterizing the atomic mass surface beyond the proton drip line via α-decay measurements of the $\pi s_{1/2}$ ground state of ^{165}Re and the $\pi h_{11/2}$ isomer in ^{161}Ta, Phys. Rev. C 86 (6) (2012) 064315, https://doi.org/10.1103/PhysRevC.86.064315.

[56] A.N. Andreyev, V. Liberati, S. Antalic, D. Ackermann, A. Barzakh, N. Bree, T.E. Cocolios, J. Diriken, J. Elseviers, D. Fedorov, V.N. Fedosseev, D. Fink, S. Franchoo, S. Heinz, F.P. Heßberger, S. Hofmann, M. Huyse, O. Ivanov, J. Khuyagbaatar, B. Kindler, U. Köster, J.F.W. Lane, B. Lommel, R. Mann, B. Marsh, P. Molkanov, K. Nishio, R.D. Page, N. Patronis, D. Pauwels, D. Radulov, Š. Šáro, M. Seliverstov, M. Sjödin, I. Tsekhanovich, P. Van Den Bergh, P. Van Duppen, M. Venhart, M. Veselský, α-decay spectroscopy of the chain ^{179}Tl$^g \rightarrow {}^{175}$Au$^g \rightarrow {}^{171}$Ir$^g \rightarrow {}^{167}$Rem, Phys. Rev. C, Nucl. Phys. 87 (5) (2013) 1, https://doi.org/10.1103/PhysRevC.87.054311.

[57] H. Kettunen, T. Enqvist, T. Grahn, P.T. Greenlees, P. Jones, R. Julin, S. Juutinen, A. Keenan, P. Kuusiniemi, M. Leino, A.P. Leppänen, P. Nieminen, J. Pakarinen, P. Rahkila, J. Uusitalo, Alpha-decay studies of the new isotopes ^{191}At and ^{193}At, Eur. Phys. J. A 17 (4) (2003) 537–558, https://doi.org/10.1140/epja/i2002-10162-1.

[58] H. Kettunen, T. Enqvist, M. Leino, K. Eskola, P.T. Greenlees, K. Helariutta, P. Jones, R. Julin, S. Juutinen, H. Kankaanpää, H. Koivisto, P. Kuusiniemi, M. Muikku, P. Nieminen, P. Rahkila, J. Uusitalo, Investigations into the alpha-decay of ^{195}At, Eur. Phys. J. A 16 (4) (2003) 457–467, https://doi.org/10.1140/epja/i2002-10130-9.

[59] J. Uusitalo, M. Leino, T. Enqvist, K. Eskola, T. Grahn, P.T. Greenlees, P. Jones, R. Julin, S. Juutinen, A. Keenan, H. Kettunen, H. Koivisto, P. Kuusiniemi, A.-P. Leppänen, P. Nieminen, J. Pakarinen, P. Rahkila, C. Scholey, α decay studies of very neutron-deficient francium and radium isotopes, Phys. Rev. C 71 (2) (2005) 024306, https://doi.org/10.1103/PhysRevC.71.024306.

[60] M.B. Smith, R. Chapman, J.F.C. Cocks, O. Dorvaux, K. Helariutta, P.M. Jones, R. Julin, S. Juutinen, H. Kankaanpää, H. Kettunen, P. Kuusiniemi, Y. Le Coz, M. Leino, D.J. Middleton, M. Muikku, P. Nieminen, P. Rahkila, A. Savelius, K.-M. Spohr, First observation of excited states in ^{197}At: the onset of deformation in neutron-deficient astatine nuclei, Eur. Phys. J. A 47 (1999) 43–47, https://doi.org/10.1007/s100500050254.

[61] U. Jakobsson, S. Juutinen, J. Uusitalo, M. Leino, K. Auranen, T. Enqvist, P.T. Greenlees, K. Hauschild, P. Jones, R. Julin, S. Ketelhut, P. Kuusiniemi, M. Nyman, P. Peura, P. Rahkila, J. Ruotsalainen, J. Sarén, C. Scholey, J. Sorri, Spectroscopy of the proton drip-line nucleus ^{203}Fr, Phys. Rev. C 87 (5) (2013) 1, https://doi.org/10.1103/PhysRevC.87.054320.

[62] A.N. Andreyev, S. Antalic, D. Ackermann, S. Franchoo, F.P. Heßberger, S. Hofmann, M. Huyse, I. Kojouharov, B. Kindler, P. Kuusiniemi, S.R. Lesher, B. Lommel, R. Mann, G. Münzenberg, K. Nishio, R.D. Page, J.J. Ressler, B. Streicher, S. Saro, B. Sulignano, P.V. Duppen, D. Wiseman, R. Wyss, α-decay of the new isotope ^{187}Po: probing prolate structures beyond the neutron mid-shell at N = 104, Phys. Rev. C 73 (4) (2006) 044324, https://doi.org/10.1103/PhysRevC.73.044324.

[63] E. Coenen, K. Deneffe, M. Huyse, P.V. Duppen, J.L. Wood, α decay of neutron-deficient odd Bi nuclei: shell-model intruder states in Tl and Bi isotopes, Phys. Rev. Lett. 54 (16) (1985) 1783–1786, https://doi.org/10.1103/PhysRevLett.54.1783.

[64] C. Scholey, M. Sandzelius, S. Eeckhaudt, T. Grahn, P.T. Greenlees, P. Jones, R. Julin, S. Juutinen, M. Leino, A.-P. Leppänen, P. Nieminen, M. Nyman, J. Perkowski, J. Pakarinen, P. Rahkila, P.M. Rahkila, J. Uusitalo, K.V. de Vel, B. Cederwall, B. Hadinia, K. Lagergren, D.T. Joss, D.E. Appelbe, C.J. Barton, J. Simpson, D.D. Warner, I.G. Darby, R.D. Page, E.S. Paul, D. Wiseman, In-beam and decay spectroscopy of very neutron deficient iridium nuclei, J. Phys. G, Nucl. Part. Phys. 31 (10) (2005) S1719–S1722, https://doi.org/10.1088/0954-3899/31/10/061.

[65] M.W. Rowe, J.C. Batchelder, T.N. Ginter, K.E. Gregorich, F.Q. Guo, F.P. Hessberger, V. Ninov, J. Powell, K.S. Toth, X.J. Xu, J. Cerny, Decay of ^{178}Tl, Phys. Rev. C 65 (5) (2002) 054310, https://doi.org/10.1103/PhysRevC.65.054310.

[66] A.N. Andreyev, M. Huyse, P. Van Duppen, C. Qi, R.J. Liotta, S. Antalic, D. Ackermann, S. Franchoo, F.P. Heßberger, S. Hofmann, I. Kojouharov, B. Kindler, P. Kuusiniemi, S.R. Lesher, B. Lommel, R. Mann, K. Nishio, R.D. Page, B. Streicher, Š. Šáro, B. Sulignano, D. Wiseman, R.A. Wyss, Signatures of the $Z = 82$ shell closure in α-decay process, Phys. Rev. Lett. 110 (24) (2013) 242502, https://doi.org/10.1103/PhysRevLett.110.242502.

[67] C. Qi, A.N. Andreyev, M. Huyse, R.J. Liotta, P. Van Duppen, R. Wyss, On the validity of the Geiger–Nuttall alpha-decay law and its microscopic basis, Phys. Lett. B 734 (2014) 203–206, https://doi.org/10.1016/j.physletb.2014.05.066.

[68] Y.A. Akovali, Review of alpha–decay data from doubly–even nuclei, Nucl. Data Sheets 84 (1) (1998) 1–114, https://doi.org/10.1006/ndsh.1998.0009.

[69] F.G. Kondev, R.V.F. Janssens, M.P. Carpenter, K. Abu Saleem, I. Ahmad, M. Alcorta, H. Amro, P. Bhattacharyya, L.T. Brown, J. Caggiano, C.N. Davids, S.M. Fischer, A. Heinz, B. Herskind, R.A. Kaye, T.L. Khoo, T. Lauritsen, C.J. Lister, W.C. Ma, R. Nouicer, J. Ressler, W. Reviol, L.L. Riedinger, D.G. Sarantites, D. Seweryniak, S. Siem, A.A. Sonzogni, J. Uusitalo, P.G. Varmette, I. Wiedenhöver, Interplay between octupole and quasiparticle excitations in ^{178}Hg and ^{180}Hg, Phys. Rev. C 62 (4) (2000) 044305, https://doi.org/10.1103/PhysRevC.62.044305.

[70] S.-C. Wu, H. Niu, Nuclear data sheets for A = 180, Nucl. Data Sheets 100 (4) (2003) 483–705, https://doi.org/10.1006/ndsh.2003.0018.

[71] P. Möller, A. Sierk, R. Bengtsson, H. Sagawa, T. Ichikawa, Nuclear shape isomers, At. Data Nucl. Data Tables 98 (2) (2012) 149–300, https://doi.org/10.1016/j.adt.2010.09.002.

[72] N.J. Stone, Table of nuclear magnetic dipole and electric quadrupole moments, At. Data Nucl. Data Tables 90 (1) (2005) 75–176, https://doi.org/10.1016/j.adt.2005.04.001.

[73] A.E. Barzakh, D.V. Fedorov, V.S. Ivanov, P.L. Molkanov, F.V. Moroz, S.Y. Orlov, V.N. Panteleev, M.D. Seliverstov, Y.M. Volkov, Laser spectroscopy studies of intruder states in ^{193,195,197}Bi, Phys. Rev. C 94 (2) (2016) 024334, https://doi.org/10.1103/PhysRevC.94.024334.

[74] J.A. Bounds, C.R. Bingham, H.K. Carter, G.A. Leander, R.L. Mlekodaj, E.H. Spejewski, W.M. Fairbank, Nuclear structure of light thallium isotopes as deduced from laser spectroscopy on a fast atom beam, Phys. Rev. C 36 (6) (1987) 2560–2568, https://doi.org/10.1103/PhysRevC.36.2560.

[75] R. Menges, U. Dinger, N. Boos, G. Huber, S. Schröder, S. Dutta, R. Kirchner, O. Klepper, T.U. Kühl, D. Marx, G.D. Sprouse, Nuclear moments and the change in the mean square charge radius of neutron deficient thallium isotopes, Z. Phys. A, Hadrons Nucl. 341 (4) (1992) 475–479, https://doi.org/10.1007/BF01301392.

[76] H.A. Schuessler, E.C. Benck, F. Buchinger, H. Iimura, Y.F. Li, C. Bingham, H.K. Carter, Nuclear moments of the neutron-deficient thallium isotopes, Hyperfine Interact. 74 (1–4) (1992) 13–21, https://doi.org/10.1007/BF02398612.

[77] A.E. Barzakh, L.K. Batist, D.V. Fedorov, V.S. Ivanov, K.A. Mezilev, P.L. Molkanov, F.V. Moroz, S.Y. Orlov, V.N. Panteleev, Y.M. Volkov, Changes in the mean-square charge radii and magnetic moments of neutron-deficient Tl isotopes, Phys. Rev. C 88 (2) (2013) 1, https://doi.org/10.1103/PhysRevC.88.024315.

[78] G. Neyens, Nuclear magnetic and quadrupole moments for nuclear structure research on exotic nuclei, Rep. Prog. Phys. 66 (4) (2003) 633–689, https://doi.org/10.1088/0034-4885/66/4/205.

[79] C.N. Davids, P.J. Woods, J.C. Batchelder, C.R. Bingham, D.J. Blumenthal, L.T. Brown, B.C. Busse, L.F. Conticchio, T. Davinson, S.J. Freeman, D.J. Henderson, R.J. Irvine, R.D. Page, H.T. Penttilä, D. Seweryniak, K.S. Toth, W.B. Walters, B.E. Zimmerman, New proton radioactivities ^{165,166,167}Ir and ^{171}Au, Phys. Rev. C 55 (5) (1997) 2255–2266, https://doi.org/10.1103/PhysRevC.55.2255.

[80] H. Kettunen, T. Enqvist, T. Grahn, P.T. Greenlees, P. Jones, R. Julin, S. Juutinen, A. Keenan, P. Kuusiniemi, M. Leino, A.P. Leppänen, P. Nieminen, J. Pakarinen, P. Rahkila, J. Uusitalo, Decay studies of ^{170,171}Au, $^{171-173}$Hg, and ^{176}Tl, Phys. Rev. C, Nucl. Phys. 69 (5) (2004) 054323, https://doi.org/10.1103/PhysRevC.69.054323.